Int. J. Electrochem. Sci., 14 **(2019)** 1208 – 1223, doi: 10.20964/2019.02.38

International Journal of
ELECTROCHEMICAL
SCIENCE
www.electrochemsci.org

Investigation of Corrosion Inhibition Efficiency of Amazonian Tree Alkaloids Extract for C38 steel in 1M Hydrochloric Media

Maxime Chevalier[1,*], *Mounim Lebrini*[1,*], *Florent Robert*[1], *Sylvain Sutour*[2], *Felix Tomi*[2], *Charafeddine Jama*[3], *Fouad Bentiss*[3,4] *and Christophe Roos*[1,*]

[1] Laboratoire Matériaux et Molécules en Milieux Agressifs, UA – UMR ECOFOG Campus de Schœlcher, 97233 Schœlcher, France
[2] Laboratoire Science Pour l'Environnement, Equipe Chimie et Biomasse, URA CNRS 2053, Université de Corse, Route des Sanguinaires, 20000-Ajaccio, France
[3] Laboratoire UMET-PSI, CNRS UMR 8207, ENSCL, Université Lille I, CS 90108, F-59652 Villeneuve d'Ascq Cedex, France
[4] Laboratoire de Catalyse et de Corrosion des Matériaux (LCCM), Faculté des Sciences, Université Chouaib Doukkali, B.P. 20, M-24000 El Jadida, Morocco
[*]E-mail: maxime.chevalier@univ-antilles.fr, mounim.lebrini@univ-antilles.fr, christophe.roos@martinique.univ-ag.fr

Received: 27 April 2018 / *Accepted:* 21 November 2018 / *Published:* 5 January 2019

The present study investigated the potential of the alkaloidic extract of *Xylopia cayennensis* used as C38 steel corrosion inhibitor in 1M HCl by electrochemical impedance spectroscopy and potentiodynamic polarization. Both methods indicated that *Xylopia cayennensis* alkaloidic extract (XCAE) acts as mixed-inhibitor with maximal efficiency up to 93% (polarization curve) and 94% (EIS measurements) for 200 mg/L. The effect of time immersion and temperature was discussed, as well as adsorption mechanism (with XPS study and adsorption isotherm). Phytochemical study was undertaken to highlight key compound responsible for the corrosion inhibition and determine major constituent of this extract, and to permit better comprehension of adsorption mechanism.

Keywords: C38 steel; *Xylopia cayennensis* extract; Adsorption-XPS; Acidic media; Corrosion inhibitor.

1. INTRODUCTION

Corrosions problems are known worldwide for many years. This corrosion concern as well private, public and industrial building. In the case of industrial process, metals can be exposed to acidic conditions like acid cleaning, acid pickling and acid descaling [1].

To protect metals and alloys like steel against this corrosion, different way exist. Employment of corrosion inhibitors is one of them. Corrosion inhibitors present different advantages like reduce cost, wide applicability, and high efficiency [2]. Various corrosion inhibitors like organic or inorganic compounds can protect metal forming a protective layer. In fact they can be adsorbed on the metal or forming an insoluble complex on the metal surface [3]. Last years, an increasing numbers of articles present inhibiting result of organic compounds. The structure of the inhibitive molecule has an important role into the efficacy of molecules. Presences of double bonds, heteroatoms like oxygen, nitrogen or sulfur can be directly correlated with a high efficiency [1, 4–16].

For safety reasons, toxicity of these compounds has to be evaluated. All compounds have to be conform to REACH directive. An important development of natural products occurred since last 15 years. The aim is to obtain molecule with the same characteristic and efficiency, but with a reduce toxicity against environment and humans. In this optics, plants extracts are very rich source of natural's compounds with a lot of different structure. Many extracts of plant can be used as green corrosion inhibitors [2, 3, 17–29].

Previous study highlight alkaloids as a class of natural molecule containing oxygen, nitrogen, and double bond inside their structure acting as natural corrosion inhibitor with high efficiency [2, 11, 30–40]. These heteroatoms and double bonds permit interaction between the inhibitor and the metal.

The aim of this study is to investigate the effect of alkaloid extracted from *X. cayennensis* alkaloid extract (XCAE) on the corrosion steel in 1M hydrochloric acid by means of electrochemical measurements and to understand how the inhibition works.

2. EXPERIMENTAL

2.1. Materials

Xylopia cayennensis is a big tree of Amazonian forest. This plant is present in South America, and especially in French Guyana. All samples collected for this study come from French Guaina's forest. The bark of *X. cayennensis* were dried in air-conditioned room for one week. Then the bark were powdered into small pieces. A specific procedure based on their acid-base properties of alkaloids is used to extract these molecules from the powder [30, 32, 41]. The alkaloidic extract of bark of *X. cayennensis* was tested with concentration range between 25 and 200 mg/L.

The electrode used for the tests are cut from cylinder of C38 steel. The composition of C38 steel, its preparation using epoxy resin, and its preparation of the working surface (ground with 180 and 1200 grit grinding papers) has been describe into previous works [30, 32].

The corrosive media (1M HCl) is prepared with the appropriate concentration of HCl 37% acid, diluted in double distilled water.

2.2. Nuclear Magnetique Resonnance (NMR)

All spectra were recorded on a Brucker 400 AVANCE spectrometer operating at 400.132 MHz for 1H NMR, and 100.623 MHz for 13C NMR. The spectrometer was equipped with a 5 mm probe,

and the solvent were deuteriated chloroform. Chemicals shifts were compared to an internal reference which one is TMS (tetramethylsilane) and measured in ppm. The coupling constants are measured in Hz. All analysis occurred at ambient temperature. Different bidimensional sequences like HMBC (Heteronuclear Multiple Bond Correlation) and HSQC (Heteronuclear Single Quantum Correlation) have been employed to complete ^{1}H and ^{13}C data.

2.3. Electrochemical measurements

VSP electrochemical measurement system (Bio-Logic) have been used for potentiodynamic polarization curves and electrochemical impedance spectroscopy (EIS). A three-electrode cell was used with C38 steel as working electrode (1 cm^2 of exposure surface), saturated calomel electrode as reference electrode, and platinium wire as counter electrode. The open circuit potential (OCP) needed 3h of immersion to be stabilized. Polarization curves were recorded from -300 to +300 mV with a scan rate of 20 mV/min. The EIS measurments were carried out at frequencies ranged from 100 kHz to 10 mHz, using ac signals of amplitude 5 mV peak to peak. All electrochemical measurements were analyzed with EC-Lab V 9.97 impedance software.

2.4. XPS studies

X-ray photoelectron spectroscopy (XPS) spectra were recorded by ESCALAB 220XL spectrometer. C38 steel disks were immersed in 1M HCl solution with XCAE (100 mg/L). All parameters for XPS study have been described into previous works [15, 30].

3. RESULTS AND DISCUSSION

3.1. Polarization curves

The study of *Xylopia cayennensis* alkaloid extract (XCAE) as corrosion inhibitor in 1M HCl media started by the polarization curves. Figure 1 presents polarization curves obtained in 1M HCl solution with or without different concentration of XCEA for C38 steel. Table 1 displays the electrochemical parameters obtained from polarization curves and the inhibition efficiency (*IE* %). The inhibition efficiency is calculated using both I_{corr} and R_p. The polarization resistance (*Rp*) values were obtained by using linear plots in the potential range ±25 mV from the corrosion potential. A good correlation ($R^2 = 0.999$) was obtained for the R_p fit.

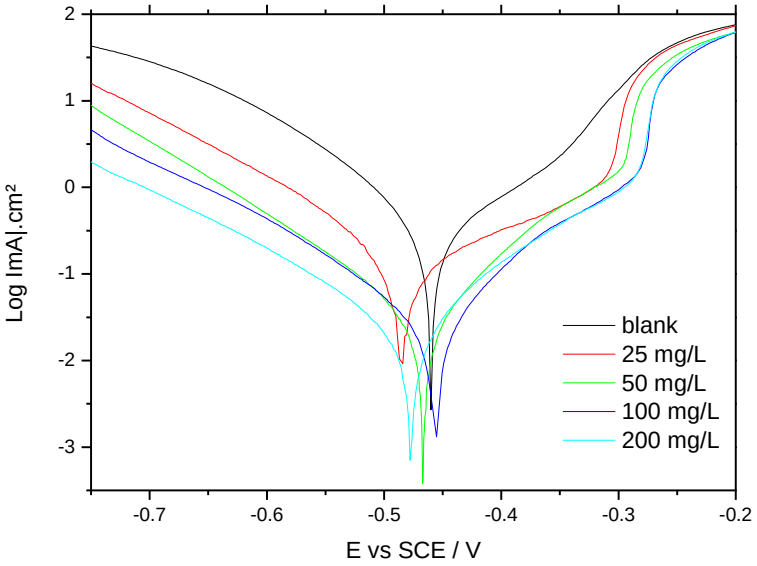

Figure 1. Polarization curves for C38 steel in 1M HCl in the absence or presence of different concentrations of XCAE at 298 K after 3h of immersion.

Table 1. Polarization parameters and inhibition efficiency for the corrosion of C38 steel in 1M HCl with or without different concentrations of XCAE at 298 K.

Concentration (mg/L)	E_{corr} (mV/SCE)	I_{corr} (μA/cm^{-2})	R_p (Ω.cm^2)	IE_{icorr} (%)	IE_{Rp} (%)
1M HCl	-460	232	76	-	-
Xylopia cayennensis					
25	-483	126	197	**46**	**61**
50	-467	34	656	**85**	**88**
100	-456	33	772	**86**	**90**
200	-478	27	1019	**88**	**93**

The current density values (both anodic and cathodic) present: decrease for all studies concentrations (Figure 1). This result indicated that the inhibitor can be classified as mixed-type inhibitor, with reduction of metal dissolution and retarding cathodic hydrogen evolution reaction, but with predominant cathodic effectiveness [31]. According to the presented results in table 1, values of E_{corr} don't shift clearly with addition of inhibitor. The magnitude (< 85 mV) of shift is well in agreement with a mixed type inhibitor [16, 42, 43]. With high over voltages (> 300 mV), in presence of XCEA, polarization curves presented an anodic breakdown potential, E_b. Polarization resistance shows constant increase with increasing concentration of XCEA. The IE_{Rp} reached 93% of efficiency for maximum concentration (200 mg/L), and shows the same trend as IE_{icorr}.

The inhibition efficiency (IE_{icorr}) increases with increasing concentration of plant extract. The maximum of efficiency (88%) is obtained at 200 mg/L.

3.2. Electrochemical impedance spectroscopy (EIS)

The inhibitive activity of *Xylopia* cayennensis is also evaluated by electrochemical impedance spectroscopy. Figure 2 shows Nyquist plots and figure 3 shows Bode plots, both for C38 steel in 1M HCl solutions without or with different concentrations of XCAE at 298 K. The Nyquist plots shows a depressed semi-circle, which one can be attributed to the surface heterogeneity. So the utilization of the constant phase element (CPE) in place of capacitance presents a better fit.

All Nyquist plots shows an increasing of loops size with increasing concentration of XCAE. The corresponding Bode plots indicated one time constant, indicating a charge transfer. Adsorption of XCAE may occur by simple surface coverage, and the molecule act as a primary interface inhibitor [44].

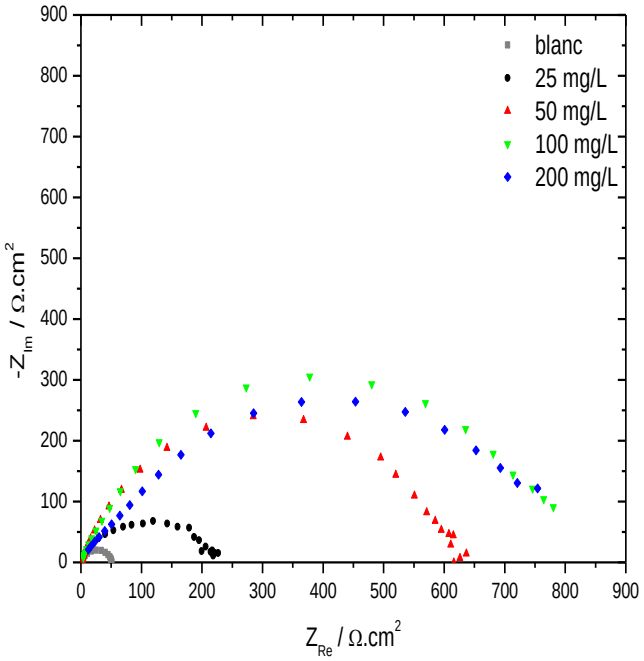

Figure 2. Nyquist plots for C38 steel in 1M HCl in absence or presence of XCEA at different concentrations at 298 K after 3h of immersion.

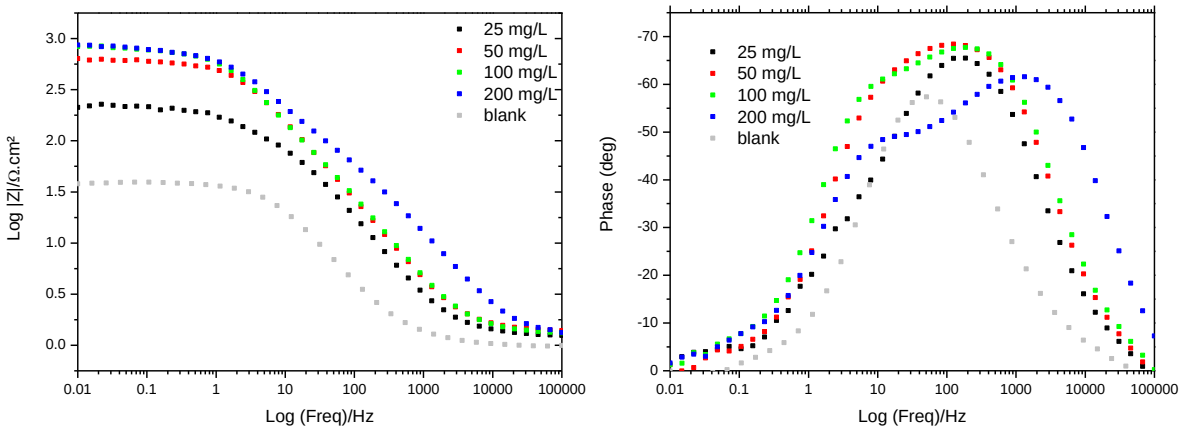

Figure 3. Bode plots for C38 steel in 1M HCl in absence or presence of XCEA at 298 K after 3h of immersion.

The equivalent circuit presented in figure 4a was used to fit the impedance data in this case. R_s represent the solution resistance, R_{ct} the charge transfer, and CPE is the constant phase element.

Figure 4. Equivalent circuit used to fit the impedance data for C38 steel in 1M HCl with or without XCAE according occures (a) one phenomenon or (b) two phenomenon.

Bode plots indicated a second time constant for the concentration of 50, 100 and 200 mg/L, which mean a second phenomenon appears. The first phenomenon at low-frequency can also be attributed to the charge transfer, and the second phenomenon at mild-frequency can be attributed to the adsorption of inhibitor on the metal surface. The equivalent circuit employed is presented in figure 4b, where R_s represent the solution resistance, R_{ct} the charge transfer, R_f the film resistance and CPE is the constant phase element. CPE is described previously, and is also represented with Q and α. Excellent fit is obtained, as seen in following figure 5, with excellent Chi-square in the order of 10^{-4}.

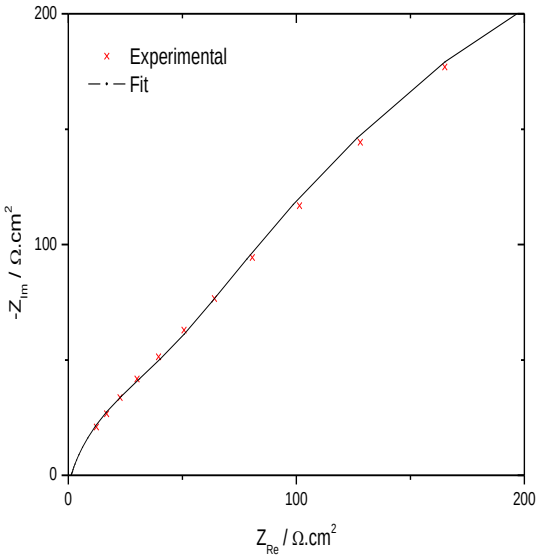

Figure 5. Nyquist plots: example for experimental data (markers) with fit data (line): zoom on high frequencies.

Data obtained from EIS for XCAE are presented in table 2**.** Inhibition efficiency is calculated with the following equation:

$$IE\ (\%) = (R_T - R_T^0) / R_T \times 100 \quad (1)$$

with $R_T = R_{ct}$, when only one phenomenon occurred and $R_T = R_{ct} + R_f$, when two phenomenon's occurred. R_T^0 is the total resistance for the blank (in absence of XCAE).

Increasing values is noted for R_{ct} with increase of concentration between 25 and 100 mg/L, and remains unchanged between 100 and 200 mg/L. Value of C_{dc} decrease with the concentration, that can be attributed to the film.

Table 2. EIS parameters and inhibition efficiency for the corrosion of C38 steel in 1M HCl with different concentrations of XCAE at 298 K.

Concentration (mg/L)	R_f (Ω.cm^2)	10^4 Q_1 (Ω^{-1}.S^n.cm^2)	α_1	C_f (μF.cm^{-2})	R_{ct} (Ω.cm^2)	10^4 Q_2 (Ω^{-1}.S^n.cm^2)	α_2	C_{dc} (μF.cm^{-2})	*IE* (%)
25	-	-	-	-	205	4.3	0.75	194	**76**
50	15	8.0	0.81	283	618	1.9	0.82	121	**92**
100	17	4.1	0.88	208	773	2.0	0.85	142	**94**
200	45	1.6	0.78	40	754	1.9	0.77	114	**94**

The inhibition efficiency from electrochemical impedance spectroscopy seems to be in good agreement with inhibition efficiency from the polarization curves study (Figure 6). Consequently, these results propose, once again, that this plant extract could serve as effective corrosion inhibitors. The results found through a lot of natural products [17, 19-28] and our results (Tables 1 and 2) advises that the plant extracts could serve as effective corrosion inhibitors. Examining the efficiency obtained with our used concentrations and those used by others natural products [17, 19-28], we can conclude that our extract is very effective associated with results of other authors, for the reason that we get almost the same efficiency with a low concentration.

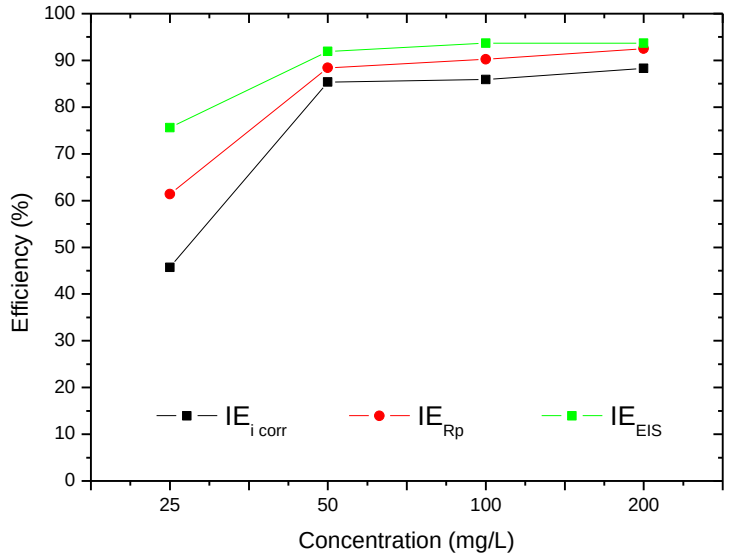

Figure 6. Efficiency variation for XCEA concentration variation calculated both polarization curves parameters (i_{corr} and R_p) and electrochemical impedance spectroscopy parameters (R_T)

The adsorption of XCAE was confirmed by study of adsorption isotherm behavior. The best fit isotherm is obtained for Langmuir isotherm (Figure 7).

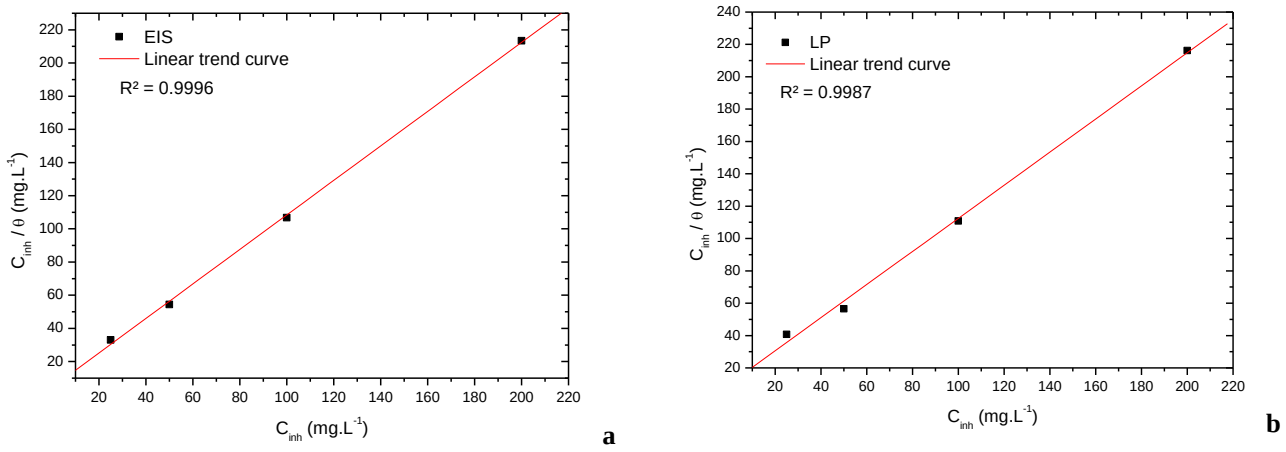

Figure 7. Langmuir adsorption plots for C38 steel in 1M HCl containing different concentrations of XCAE at 298 K: (a) data from EIS measurements and (b) data from linear polarization curves.

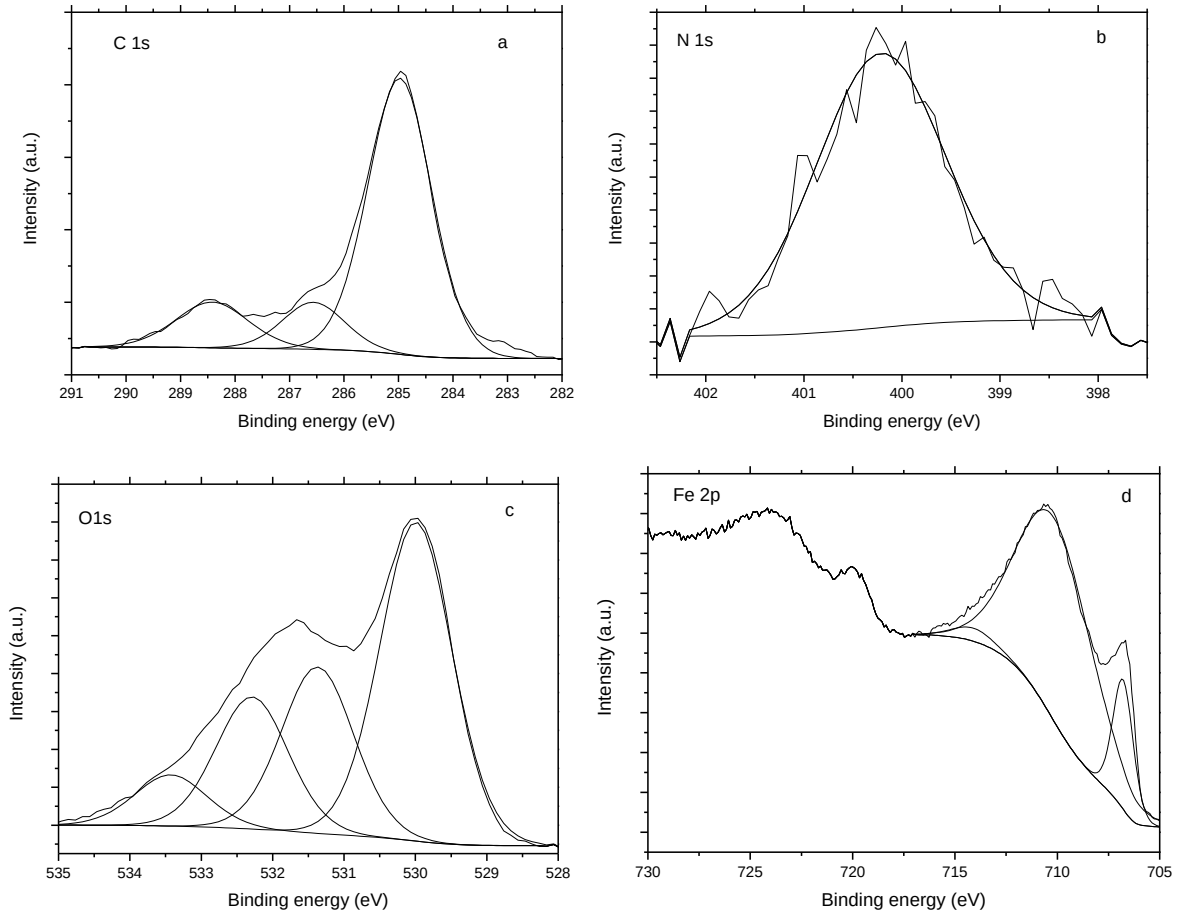

Figure 8. XPS deconvolution for C1s, O1s, N1s and Fe 2p for C38 steel surface treated with XCEA in 1M HCl at 298 K.

This result indicates that the adsorption take place with a single-layer mechanism on the surface metal. This mechanism can explain the access limitation of aggressive media for the metal surface, and its inhibition power. Moreover, Langmuir isotherm is based on no interaction between molecules on this surface. But in presence of alkaloidic extract (so in presence of complex heteroatoms), it's is few probably that there is no interactions take place.

To continue the study of adsorption mechanisms, analyzes with X-ray photoelectron spectroscopy take place. Characteristics spectra C1s, N1s, O1s, and Fe2p are presented in figure 8 for C38 steel exposed to aggressive media with XCAE. Deconvolution for all spectra are analyzed, like method presented in previous work [30].

The deconvolution of C1s spectrum of C38 steel with XCAE is fitted with three components (Figure 8a). Major component at a binding energy ≈ 285 eV can be attributed to bonds C-C, C=C, and C-H aromatics bonds [45]. Second component at 286.5 eV can represent bond between carbon and nitrogen like C-N [45]. The third component at 288.4 can represented bonds like O-CH_3 [2]. These first results indicate the presence of heteroatoms at the surface of C38 steel. The alkaloid extract is well adsorbed at the metal surface.

Figure 8b presents the N1s spectrum. The spectrum shows a major peak centered at 400 eV. This peak seems to be large and presents a lot of oscillations. It's probably a combination of many peaks. Three components can be envisaged like currently encountered in other studies with similar conditions [13,15,45,46]. The major component at 400.2 can be attributed to Fe-N bond. Two other components can be considered. One component at ≈ 399.5 eV could be attributed to C-N bonds, and a third component at ≈ 401 eV could be attributed to bond between carbon and protonated nitrogen N^+. The alkaloids in this extract could be chemically adsorbed with presence of Fe-N bonds, but also physically adsorbed because of presence of protonated nitrogen near negatively charged metal surface.

The O1s spectrum (Figure 8c) could be fitted into four peaks. The major peak, at ≈ 530 eV could be attributed at O^{2-} bond with iron, like into FeO, Fe_2O_3 and Fe_3O_4 [47]. The second peak at 531.4 can be attributed to OH^-, and can represented compounds like FeOOH and $Fe(OH)_3$ [45]. The third and fourth peak at ≈532.8 and 533.5 eV can be attributed to oxygen bond into water, adsorbed on the metal surface [2].

Fe2p spectrum (Figure 8d) presents two double peaks at 711 ($Fe2p_{3/2}$) and 724 eV ($Fe2p_{1/2}$) approximatively, which one is characteristic of oxidative surface metal. Peak at 720 eV can be ascribed to the satellites of ferric compounds [45]. The deconvolution of $Fe2p_{3/2}$ spectrum consists of three distinct peaks. The first peak at ≈ 707 eV is attributed to Fe^0 (metallic iron). The second and major component at ≈ 711 eV can be attributed to Fe^{3+} species, which consists of FeO, Fe_2O_3, and FeOOH. The third and very minor component at 714 eV is ascribed to presence of $FeCl_3$ in very small concentration.

These observations permit to conclude first: the metal is oxidized in this aggressive media; then: interactions take place between XCAE and the metal surface. Molecules of XCAE seem to be adsorbed on the metal surface because of evidence of their presence. Moreover, this adsorption seems to be double: physical type and also chemical type.

3.3. Effect of immersion time and temperature

To continue the study of XCAE as corrosion inhibitor, the immersion time was studied. This parameter permits to appreciate the stability of inhibitor on the metal surface. Only results obtained by EIS measurements was presented. Figure 9 presents the Nyquist diagrams at different immersion time with 50 mg/L of XCAE in 1M HCl at 298 K. These results are compared to the same immersion time without XCAE (blank) in order to calculate the inhibition efficiency. The trend of inhibition efficiency as a function of time immersion is presented in figure 10. The data obtained show a stable efficiency during the experiment, with a slight decrease at 6h and 18h immersion time. XCAE can be considered as a stable inhibitor all along the experimentation. This stability can be attributed to the adsorptive film on the metal surface. This adsorptive film could be aggressed between 6 and 18h, and could become more compact after 24h [48].

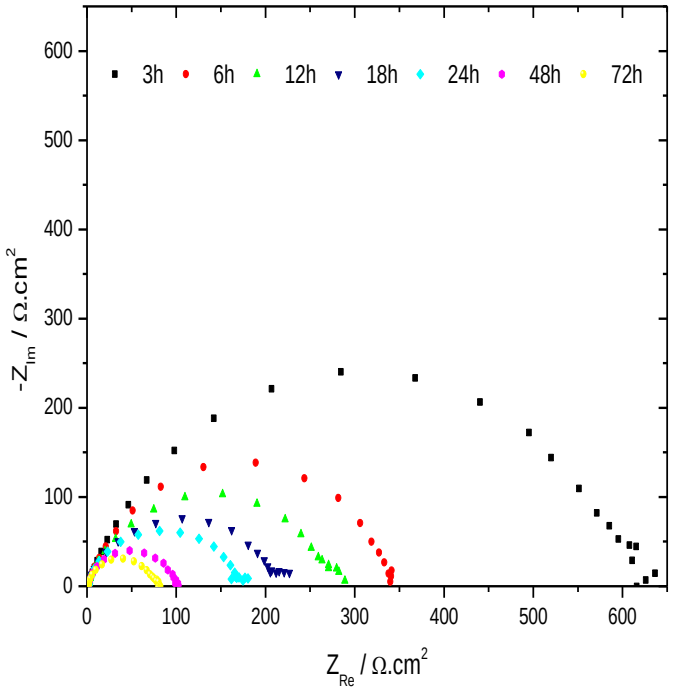

Figure 9. Nyquist plots for C38 steel in 1M HCl with 50 mg/L of XCEA at different immersion times at 298 K.

To complete the study of the XCAE, the alkaloidic extract was tested in range of temperature between 298 and 328 K. Figure 11 presents Nyquist diagrams for C38 with 50 mg/L of XCAE at different temperatures (298-328 K) in 1M HCl. Nyquist diagram shows that R_{ct} decrease with increase of temperature. Compare to blank values, the inhibition efficiency stay stable in the range of temperature studied with a maximum efficiency of 95% for 308 K. The trend of inhibition efficiency as a function of temperature immersion is presented in figure 12. All values for inhibition efficiency are over 89%.

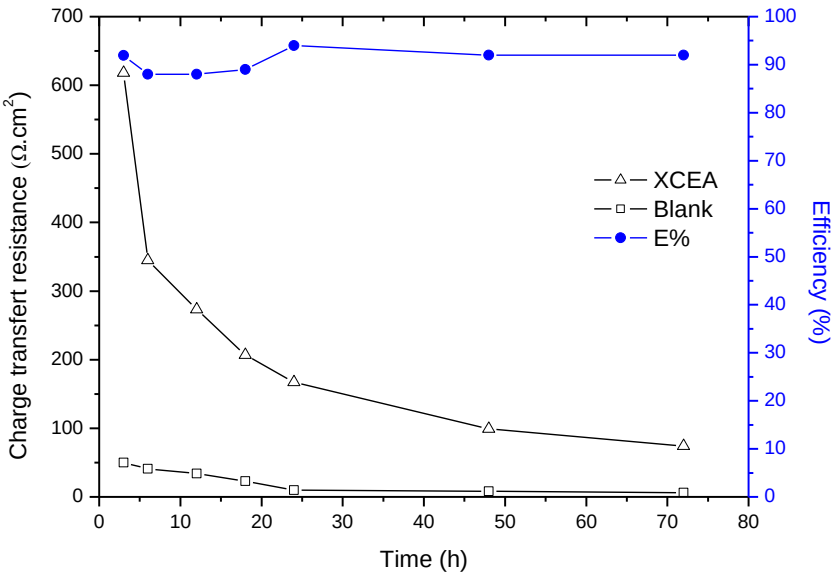

Figure 10. Corrosion inhibition efficiency for XCEA at 50 mg/L as a function of immersion time.

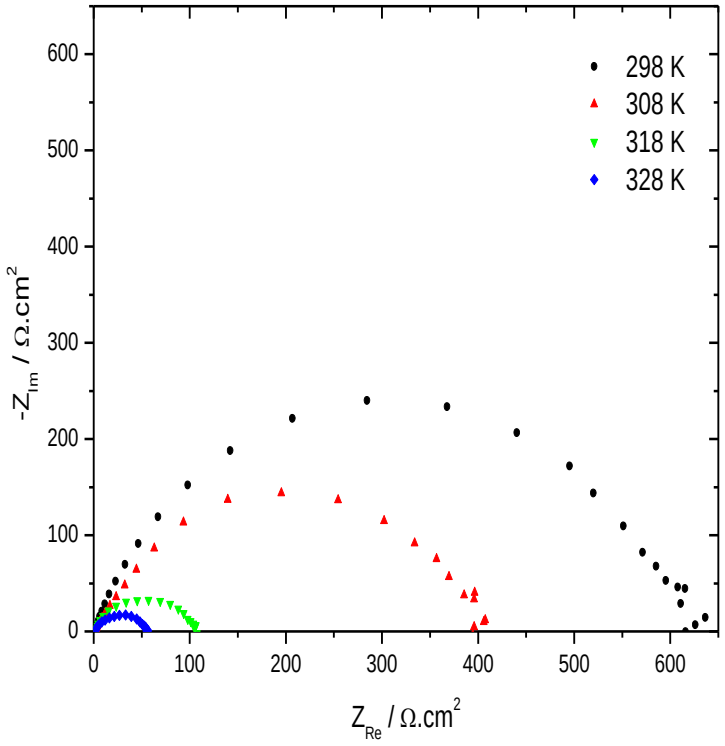

Figure 11. Nyquist plots for C38 steel in 1M HCl with 50 mg/L of XCEA at different temperatures after 3h of immersion.

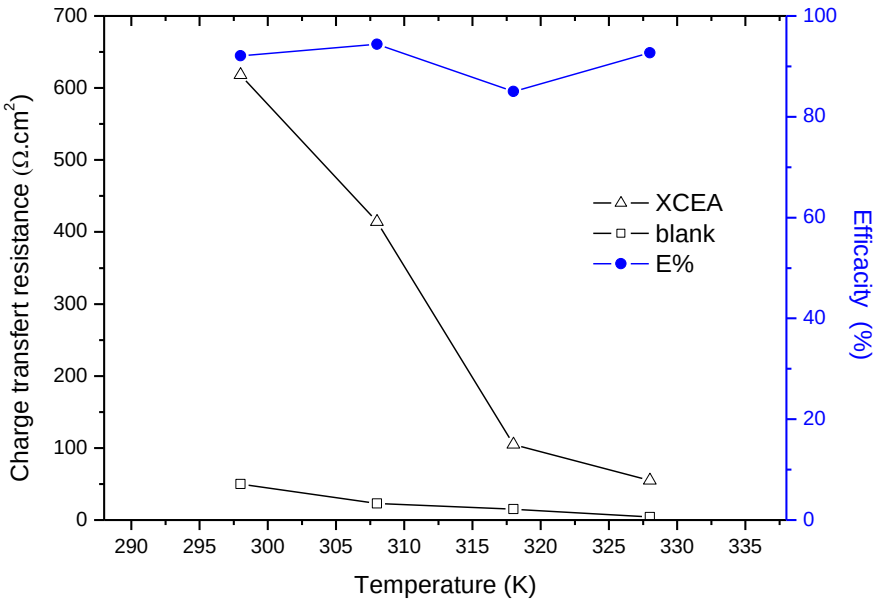

Figure 12. Corrosion inhibition efficiency for XCEA at 50 mg/L as a function of temperature.

3.4. Isolation, identification, and EIS measurements of major compound

As seen previously in this study, XCAE acts as a good corrosion inhibitor for C38 steel in acidic condition. To continue this study, the major compound of the total extract was isolated and studied by electrochemical measurements. This study permits its comparison with the total extract.

Total alkaloidic extract of *Xylopia cayennensis* was fractioned on open chromatography column. The stationary phase used was silica gel (60 then 200 µm), with add of 10% sodium bicarbonate for better separation. Eluent was different gradient of chloroform/ethyl acetate/methanol. Every tube were analyzed with thin layer chromatography and UV box (256 and 365 nm). Six fractions were obtained after grouping. All six factions as well as total extract XCAE were analyzed by ^{1}H and ^{13}C NMR.

Study of different NMR spectra of fractions and XCAE reveals that the second fraction contained a major compound with high purity and represents 16.5 % of the total extract. By comparison of ^{13}C NMR data recorded with those from the literature, this major compound was identified as discretine with the followed IUPAC name (13aS)-2,10,11-trimethoxy-6,8,13,13a-tetrahydro-5H-isoquinolino[2,1-b]isoquinolin-3-ol [49]. The structure of discretine and its ^{13}C NMR spectra data are detailed in figure 13. Study of the corrosion inhibition efficiency of discretine with its percentage in the extract was carried out by electrochemical impedance spectroscopy. Figure 14 presents the Nyquist plots for C38 steel in 1M HCl with or without XCAE or discretine. Comportment of discretine seems to be identical to XCAE. Efficiency for discretine at 16.5 mg/L is equal to XCAE at 50 mg/L with 92% as seen in table 3. It is possible to think that a competitive phenomenon occurs in this extract. Moreover, efficiency of discretine at 16.5 mg/L is near to be efficiency of XCAE at 100 mg/L, what support this possible competitive phenomenon.

As seen as XCAE study, adsorption seems to be both chemical and physical. Physical adsorption take place through electrostatics bonds between charged surfaces and charges molecules.

Protonation of the major compound of XCAE in acidic media is studied. Discretine is derived from tetrahydroisoquinoline ring, which one presents pKa equal to 10.8. In this ring, no way for conjugation because of distance between nitrogen, aromatic rings and heteroatoms. Basicity of discretine should be just near basicity of tetrahydroisoquinoline ring. In the studied pH, the discretine is protonated like presented in figure 15.

a **b**

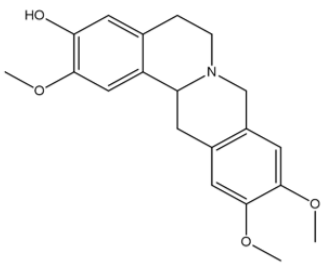

n°C	δ_C (ppm) ; mult.
1	107,8 ; CH
2	145,4 ; qC
3	144,4 ; qC
4a	127,1 ; qC
5	28,5 ; CH_2
6	51,2 ; CH_2
8	58 ; CH_2
8a	125,8 ; qC
9	109 ; CH
10	147,5 ; qC
11	147,7 ; qC
12	111,3 ; CH
12a	126 ; qC
13	36,1 ; CH_2
13a	59,6 ; CH
13b	128,6 ; qC
H3CO-2	56.6 ; CH_3
H3CO-10	56.4 ; CH_3
H3CO-11	56.5 ; CH_3

Figure 13. Major compound of XCAE: (a) structure of discretine and (b) its ^{13}C NMR spectral data.

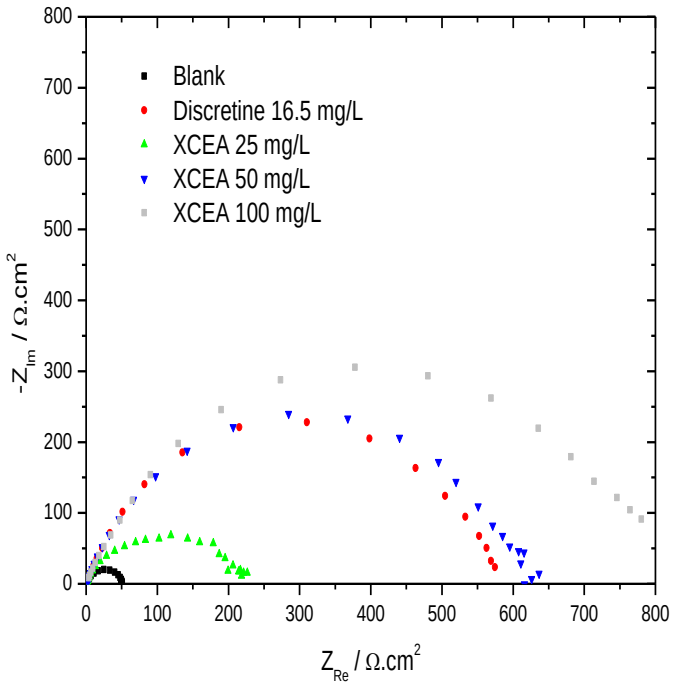

Figure 14. Nyquist plots for C38 steel in 1M HCl solutions without or with different concentrations of XCEA and discretine at 16.5 mg/L at 298 K after 3h of immersion.

Table 3. Efficiency of discretine and XCAE at different concentration on corrosion of C38 steel at 298 K.

	R_T (Ω.cm2)	*IE* (%)	*C (mg/L)*
Discretine	585,2	**92**	16,5
XCAE	205	**76**	25
XCAE	618	92	50
XCAE	790	94	100

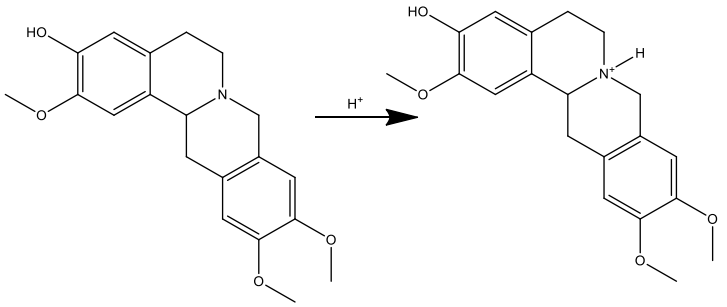

Figure 15. Protonation of discretine at pH study (pH ≈ 0).

4. CONCLUSIONS

Xylopia cayennensis alkaloid extract was studied here as a corrosion inhibitor for C38 steel in 1M HCl solution. This study shows that this extract can be considered as I) efficiency from 50 mg/L; II) stable from 3 until 72h; and III) stable in the range of temperature tested (298 – 328 K). The extract was adsorbed on the metal surface, and this adsorption seems to be both chemically and physically. Moreover, to complete the study of *Xylopia cayennensis* alkaloid extract, phytochemical study was undertaken. Major compounds was isolated and identified as discretine and was considered efficient at the concentration tested.

ACKNOWLEDGEMENT
This work was supported by European Union through FSE, and by Centre National d'Etudes Spatiales (CNES).

References

1 G. Schmitt, *Br. Corros. J.,* 19 (1984) 165.
2 N. El Hamdani, R. Fdil, M. Tourabi, C. Jama and F. Bentiss, *Appl. Surf. Sci.,* 357 (2015) 1294.
3 M. Mobin and M. Rizvi, *Carbohydr. Polym.,* 160 (2017) 172.
4 M. Finšgar and J. Jackson, *Corros. Sci.* 86 (2014) 17.
5 M. Lebrini, G. Fontaine, L. Gengembre, M. Traisnel, O. Lerasle, N. Genet, *Corros. Sci.,* 51 (2009) 1201.
6 F. Bentiss, M. Lebrini, H. Vezin, F. Chai, M. Traisnel and M. Lagrené, *Corros. Sci.,* 51 (2009) 2165.
7 M. Lebrini, M. Lagrenée, H. Vezin, L. Gengembre and F. Bentiss, *Corros. Sci.,* 47 (2005) 485.
8 M. Lebrini, M. Traisnel, M. Lagrenée, B. Mernari and F. Bentiss, *Corros. Sci.,* 50 (2008) 473.

9 N. Labjar, M. Lebrini, F. Bentiss, N.-E. Chihib, S. El Hajjaji and C. Jama, *Mater. Chem. Phys.*, 119 (2010) 330.
10 M. Lebrini, F. Robert, H. Vezin and C. Roos, *Corros. Sci.*, 52 (2010) 3367.
11 M. Lebrini, F. Bentiss, H. Vezin and M. Lagrenée, *Corros. Sci.*, 48 (2006) 1279.
12 M. Lebrini, M. Traisnel, L. Gengembre, G. Fontaine, O. Lerasle and N. Genet, *Appl. Surf. Sci.*, 257 (2011) 3383.
13 M. Lebrini, M. Lagrenée, M. Traisnel, L. Gengembre, H. Vezin and F. Bentiss, *Appl. Surf. Sci.*, 253 (2007) 9267.
14 M. Lebrini, F. Bentiss, H. Vezin and M. Lagrenée, *Appl. Surf. Sci.*, 252 (2005) 950.
15 M. Outirite, M. Lagrenée, M. Lebrini, M. Traisnel, C. Jama, H. Vezin and F. Bentiss, *Electrochim. Acta*, 55 (2010) 1670.
16 M. Lebrini, M. Lagrenée, H. Vezin, M. Traisnel and F. Bentiss, *Corros. Sci.*, 49 (2007) 2254.
17 E. Ituen, O. Akaranta, A. James and S. Sun, *Sustain. Mater. Technol.*, 11 (2017) 12.
18 A. Ehsani, M.G. Mahjani, M. Hosseini, R. Safari, R. Moshrefi and H. M. Shiri, *J. Colloid Interface Sci.*, 490 (2017) 444.
19 M. Jokar, T.S. Farahani and B. Ramezanzadeh, *J. Taiwan Inst. Chem. Eng.*, 63 (2016) 436.
20 A.Y. El-Etre and A.I. Ali, *Chinese J. Chem. Eng.*, 25 (2017) 373.
21 J. Bhawsar and P.K.P. Jain , *Alexandria Eng. J.*, 54 (2015) 769.
22 K. Boumhara, M. Tabyaoui, C. Jama and F. Bentiss, *J. Ind. Eng. Chem.*, 29 (2015) 146.
23 A.S. Yaro, A.A. Khadom and R.K. Wael, *Alexandria Eng. J.*, 52 (2013) 129.
24 N.A. Odewunmi, S.A. Umoren and Z.M. Gasem, *J. Environ. Chem. Eng.*, 3 (2015) 286.
25 M. Ramananda Singh, P. Gupta and K. Gupta, *Arab. J. Chem.*, (2015).
26 P. Mourya, S. Banerjee and M.M. Singh, *Corros. Sci.*, 85 (2014) 352.
27 G. Ji, S. Anjum, S. Sundaram and R. Prakash, *Corros. Sci.*, 90 (2015) 107.
28 A.F Alhosseini and M. Noori, *Measurement*, 94 (2016) 787.
29 M.K. Bagga, R. Gadi, O.S. Yadav, R. Kumar, R. Chopra and G. Singh, *J. Environ. Chem. Eng.*, 4 (2016) 4699.
30 M. Chevalier, F. Robert, N. Amusant, M. Traisnel, C. Roos and M. Lebrini, *Electrochim. Acta*, 131 (2014) 96.
31 M. Faustin, A. Maciuk, P. Salvin, C. Roos and M. Lebrini, *Corros. Sci.*, 92 (2015) 287.
32 M. Lebrini, F. Robert, A. Lecante and C. Roos, *Corros. Sci.*, 53 (2011) 687.
33 M. Lebrini, F. Robert and C. Roos, *Int. J. Electrochem. Sci.*, 5 (2010) 1698.
34 A. Lecante, F. Robert, M. Lebrini and C. Roos, *Int. J. Electrochem. Sci.*, 6 (2011) 5249.
35 M. Lebrini, F. Robert, P.A. Blandinières and C. Roos, *Int. J. Electrochem. Sci.*, 6 (2011) 2443.
36 P.B. Raja, A.K. Qureshi, A. Abdul Rahim, H. Osman and K. Awang, *Corros. Sci.*, 69 (2013) 292.
37 P. Bothi Raja and M.G. Sethuraman, *Mater. Lett.*, 62 (2008) 1602.
38 A. Lecante, F. Robert, P. a. Blandinires and C. Roos, *Curr. Appl. Phys.*, 11 (2011) 714.
39 M. Lebrini, F. Robert and C. Roos, *Int. J. Electrochem. Sci.*, 6 (2011) 847.
40 M.I. Awad, *J. Appl. Electrochem.*, 36 (2006) 1163.
41 J. Bruneton, *Pharmacognosie, Phytochimie Plantes médicinales, Tec & Doc Lavoisier, 4e édition* (2008).
42 H.M. Abd El-Lateef, *Corros. Sci.*, 92 (2015) 104.
43 O.L.R. JR., *Corrosion*, 31 (1975) 413.
44 H. Fischer, *Werkstoffe Und Korrosion*, 23 (1972) 445.
45 F. Bentiss, C. Jama, B. Mernari, H. El Attari, L. El Kadi, M. Lebrini, M. Traisnel and M. Lagrenée, *Corros. Sci.*, 51 (2009) 1628.
46 M. Lebrini, Synthèses et études physicochimiques de nouveaux thiadiazoles inhibiteurs de corrosion de l'acier en milieu acide, *Thesis, Université de Lille* (2005).
47 P. Bommersbach, C. Alemany-Dumont, J.P. Millet and B. Normand, *Electrochim. Acta*, 51

(2005) 1076.
48 X. Li, S. Deng, H. Fu and G. Mu, *Corros. Sci.*, 51 (2009) 620.
49 E.V. Costa, L.M. Dutra, A. Nepel and A. Barison, *Biochem. Syst. Ecol.*, 51 (2013) 331.
50 M. Chevalier, C. Roos, F. Tomi, S. Sutour and M. Lebrini, *ECS Trans.*, 64 (2015) 1.